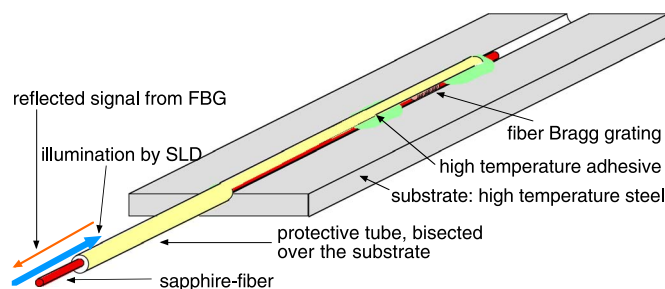# High-Temperature Strain Sensing Using Sapphire Fibers With Inscribed First-Order Bragg Gratings

**T. Habisreuther**
**T. Elsmann**
**A. Graf**
**M. A. Schmidt**

# High-Temperature Strain Sensing Using Sapphire Fibers With Inscribed First-Order Bragg Gratings

**T. Habisreuther,[1] T. Elsmann,[1] A. Graf,[1] and M. A. Schmidt[1,2,3]**

[1]Leibniz Institute of Photonic Technology, 07745 Jena, Germany
[2]Abbe Center of Photonics and the Faculty of Physics, Friedrich-Schiller-Universität Jena,
07743 Jena, Germany
[3]Otto Schott Institute of Materials Research, 07743 Jena, Germany

**Abstract:** Strain sensor designs and strain measurements based on single-crystal sapphire fibers with inscribed first-order fiber Bragg gratings for applications up to 600 °C are presented. We report on all the details of two different sensor designs; for instance, we show that the resolution of multimode sapphire fiber Bragg grating (SFBG) strain sensors is about $\Delta l/l = 10^{-5}$ (10 $\mu$strain), which is comparable with state-of-the-art high-temperature sensors. We apply our sensors for the determination of the thermal expansion coefficients of high-temperature steel alloys, showing a good match to known values. Hence, we believe that SFBG sensors may represent a promising alternative to currently used non-optic-based strain-detecting devices.

**Index Terms:** Fiber gratings, fiber optic systems, sensors.

## 1. Introduction

Higher operation temperatures in power plants [1] or gas turbines [2] allow an increase in the efficiency of such infrastructures and, thus, a reduction of $CO_2$ emissions. In particular, the materials and components in such installations are highly stressed if very high temperatures are applied requiring online monitoring and materials with improved properties [3]. Mechanical strain at high temperatures leads to material fatigue, and thus structural health monitoring (SHM) with adapted new types of sensors [4], [5] is a key issue for a long-term safe operation in such a crucial environment. One of the important tasks of SHM is precise strain diagnostics. At room temperature, many of the used strain sensors are in fact strain gauges. First, strain gauges based on Pt-W alloys as sensing elements for application at higher temperatures are available [6]. This clearly emphasizes that developing strain gauges for long term high temperature application is of key interest in many applications.

Due to their flexibility, fiber optic strain sensors are of great importance and are commercial in various implementations [7]–[9]. In particular, Fiber Bragg sensors provide a unique combination of high sensitivity and high dynamic range. They are of particular interest for industrial application since they can be applied in harsh environments [10] such as high temperature, radiation,

pressure, hydrogen atmosphere, or civil construction [11]. In addition, they are not influenced by electromagnetic fields. Spectral multiplexing of these sensors allows monitoring strain at various locations in the installations. However, if temperatures above 200 °C are considered, the application of conventional fiber Bragg gratings is limited, because standard FBGs inscribed by the ultraviolet (UV)-technique start bleaching. Regenerated FBGs [12], [13] are stable at temperatures in the range of 1000 °C, but due to the fabrication process, these sensors are very brittle. Hence, increasing the working temperature of fiber optics sensors is still a challenge.

Single crystalline sapphire fibers with a melting point above 2000 °C are a promising candidate for optical high temperature sensors. High temperature strain sensing using sapphire fiber Fabry–Pérot sensors was demonstrated [14]. The thermal stability of sapphire Fiber Bragg gratings (SFBG) was tested well above 1200 °C [15], [16], and it was shown that they even can be applied at 1900 °C for temperature sensing [17]. It was shown that these gratings are also suitable to detect strain [18]. In this paper we will present first designs of SFBG based strain sensors operating up to 600 °C. We will discuss the performance of SFBG for strain sensing and show, as an example, an application of our sensor for measuring the thermal expansion of various steels at high temperature.

## 2. Sensor Fabrication

Our idea for fiber-based high temperature strain sensors is first order fiber Bragg gratings inscribed single crystalline sapphire fibers. The crystal c-axis is parallel to the fiber axis (c-axis oriented). The commercial fiber(Micro Materials Inc.) is in fact a single material sapphire rod with a diameter of 100 $\mu$m and a length of 1 m which is so thin that the material can be bend in a similar way as silica glass fibers. Total-internal reflection inside the sapphire is provided by total internal reflection at the sapphire-air interface. Due to the comparably large diameter, the fiber is highly multimode. The sapphire fiber Bragg gratings (SFBG) were inscribed into the crystalline fiber using a fs Ti: Sapphire laser (details on the inscription of were reported in [19]).

An important point is that strain sensors require a force-fit connection of the sensing element to the object under investigation. For high temperature applications conventional adhesives based on organic chemistry can obviously not be used. One also has to consider that sapphire fibers have an air cladding, and thus the refractive index of the adhesive has to be lower than the index of sapphire($n_{\text{sapphire}} = 1.75$ at 1.55 $\mu$m wavelength) to ensure efficient light guidance via total internal reflection.

Various high temperature adhesives are commercial available. The curing process most of these adhesive requires a specific thermal treatment that can last for several days. Applying an SFBG as strain sensor on-site therefore seems not practicable in the most applications, as applying the specific temperature treatment would require an immense additional installation effort and presumably a shutdown of the plant.

Therefore we tested several sensor designs to fabricate a sensor that can be applied for example by spot welding. For the first design, the sapphire fiber was fixed inside an Inconel tube using a ceramic glue with filling particles with a dimensions of approx. 1 $\mu$m. The small particles seem to be beneficial from the operation point of view, as it can be anticipated that such particles will not impose high punctual stress on the sapphire fiber during the curing procedure, thus preventing failure of the sensor.

A second approach is shown in Fig. 1. The sapphire fiber is mechanically protected using a steel tube which is half cut on a length of about 4 cm (yellow tube in Fig. 1). The protective tube and the sapphire fiber were fixed by high temperature adhesive, whereas the SFBG is in-between the two gluing spots. The base steel plate (20*50*1 mm$^3$) with the V-groove having the sensor inside thus acts as sensor pad which can be spot-welded to any device under investigation.

## 3. Signal Processing

In general fiber Bragg gratings react on temperature and strain by a shift of the resonance wavelength (here the wavelength at which constructive interference of the forward and
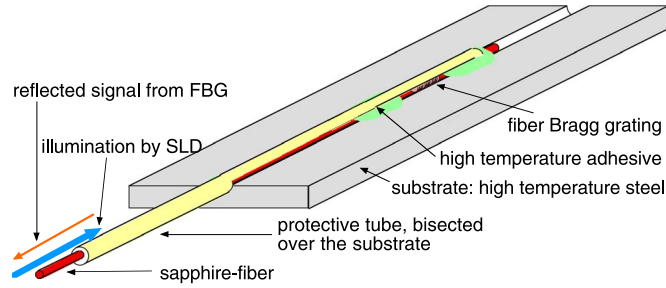
Fig. 1. Design of an SFBG strain sensor. The sapphire fiber is inserted into a partially half-cut metallic protective tube that, together with the fiber, is fixed to the steel plate via high-temperature adhesive. The grating is located in between the two gluing spots.
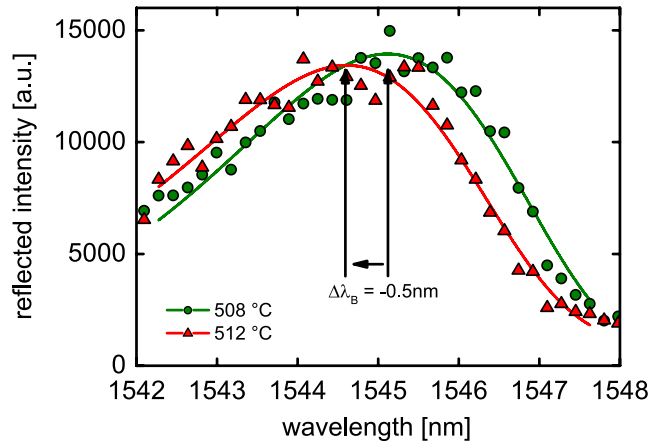


Fig. 2. Asymmetric reflection peak of the SFBG. The symbols represent the measured reflection intensities in arbitrary units. The solid lines are the fitted peak functions using (2). Strain release in the fiber causes a shift of the Bragg wavelength of 0.5 nm to lower values marked by arrows.

backward propagating waves inside the grating leads to a reflection peak) $\Delta\lambda\varepsilon_T$ [20]

$$\Delta\lambda\varepsilon_T = \Delta\lambda_T + \Delta\lambda\varepsilon = \lambda_B \bullet \Delta T \bullet (\alpha_S + \alpha_n) + \lambda_B \bullet (1 - p) \bullet \varepsilon \qquad (1)$$

where $\lambda_B$ is the Bragg wavelength (wavelength of maximum reflection); $\Delta\lambda\varepsilon_T$ and $\Delta\lambda\varepsilon$ are the spectral shifts caused by temperature or strain, respectively; $\alpha_S$ is the thermal temperature expansion coefficient of the fiber; $\alpha_n$ is the thermo-optic coefficient; $p$ is the coefficient of the photo elastic interaction; and $\varepsilon$ is the applied strain.

The multimode character of sapphire fiber used here results in a broad asymmetric peak in the respective reflection spectrum (see Fig. 2), which is in fact the envelope of all modes reflected by the SFBG. To determine the Bragg wavelength from a practical and engineering perspective, an empirical asymmetric peak function was fitted to the reflection spectrum [16]

$$I = I_0 + A \bullet \exp[(-\exp(-z)) - z + 1], \ z = \frac{(\lambda - \lambda_B)}{w}. \qquad (2)$$

The typical fit tolerance we observe here for the Bragg wavelength fitting a single spectrum is $\Delta\lambda_B \pm 80$ pm. It was shown in [21] that the fit performance can be improved by averaging several fitted values of $\Delta\lambda_B$ (e.g., averaging 20 spectra reduces the tolerance down to $\Delta\lambda_B \pm 10$ pm). A typical value for the peak with is 7 nm $\pm$ 0.1 nm. For illumination, we use a SLD light source with a Gaussian like intensity distribution in the spectral range from 1510 to 1590 nm, a commercial FBG interrogator (Ibsen Photonics) modified by a 50 $\mu$m graded index (GI) fiber entrance, a
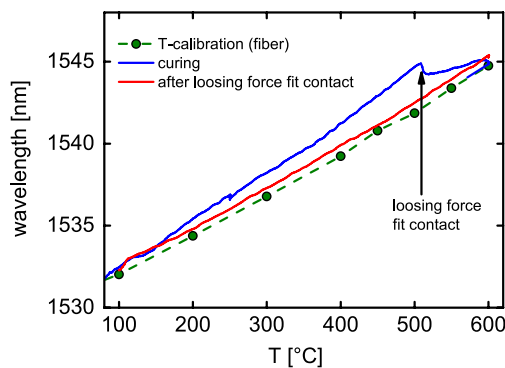
Fig. 3. Temperature dependence (green point: measurements) of the Bragg reflection peak of the SFBG (blue line: continuous data acquisition) of the sensor during curing and (red line, continuous data acquisition) of an additional heating step after loosing the force-fit contact. The vertical black arrow indicates the temperature at which the contact was lost.
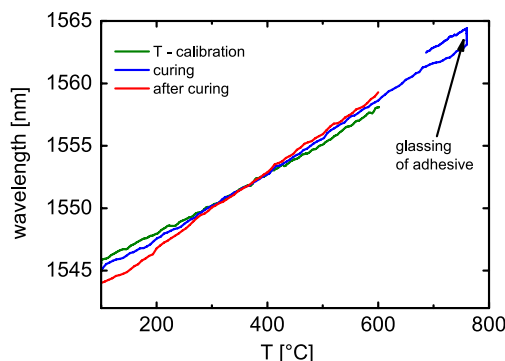
Fig. 4. Temperature dependence of the SFBG strain sensor (design shown in Fig. 1) using a glass adhesive. (Green line) Temperature dependence of the fiber. (Blue line) Curing of the adhesive. (Red line) After curing.

50 $\mu$m GI fiber-optic $Y$-coupler, and a 50 $\mu$m GI launch fiber with a length of 100 m as mode scrambler [19]. Combining the air clad multimode sapphire fiber with the commercially available 50 $\mu$m GI multimode fibers was leading to a stable configuration that allows the processing to obtain the Bragg wavelength from the measurement spectra.

## 4. Temperature and Strain Dependence of Sapphire FBG

The thermal expansion coefficient and the thermo-optic coefficient (at 600 nm) of sapphire are $\alpha_S \approx 7.2 \bullet 10^{-6}/\text{K}$ [22] and $\alpha_n \approx 12.6 \bullet 10^{-6}/\text{K}$ [18], respectively. From this data the temperature dependence of SFBGs at a wavelength of 1.55 $\mu$m calculates to $\Delta\lambda_B/\Delta T = 30.5$ pm/K.

As it can be seen from Figs. 3 and 4, the temperature dependence can be approximated by a linear function in the temperature range from 100 °C to 600 °C. Experimentally we observed variations in temperature dependence from fiber to fiber from 24 pm/K to 30 pm/K (e.g., the fiber of Fig. 3 shows a temperature dependence of 24.6 pm/K whereas the fiber in Fig. 4 shows 24.1 pm/K). The origin of these variations is not understood, yet. A specific temperature calibration for each grating has to be performed. For larger temperature ranges a parabolic temperature dependence is observed [17], [23].

Mihailov *et al.* showed in the first publication on sapphire FBG as strain sensor [18] that the response of the Bragg wavelength shift on strain is 1.4 pm/$\mu$strain, and they calculated for the coefficient of the photo elastic interaction (1) $p = 0.13$ [18].

From these data, it can be seen that the cross sensitivity between temperature and strain in sapphire fibers needs to be accurately considered. As example, a change in temperature of 1 K corresponds to an applied strain of about 20 $\mu$strain. Trying to detect strain of 10 $\mu$strain will require stabilizing or determining the temperature with a resolution of 0.5 K, which, from a practical point of view, is a requirement being though but possible to fulfill in the temperature range below 700 °C either by conventional temperature sensors or multiplexed SFBGs. The overall resolution to determine the Bragg reflection wavelength is 19 pm, giving a minimum possible detectable strain of 10 $\mu$strain.

In comparison to fused silica, sapphire fibers show a 2.5 to 3 times higher temperature sensitivity, mainly caused by larger the thermal expansion of sapphire. In addition, the strain sensitivity of SFBG is enhanced by about 10% caused by the smaller value of *p*.

## 5. Strain Sensors Based on Sapphire FBG

### 5.1. Analysis of the First Sensor Design

Fig. 3 shows the shift of the Bragg reflection wavelength as function of temperature for the first sensor design with the fiber fixed in an Inconel tube. The green symbols represent the temperature calibration of the fiber (the dashed line is a guide for the eye), the blue curve was measured during curing the ceramic adhesive and the heating to 600 °C, whereas the red curve was taken in a subsequent heating cycle.

The ceramic adhesive based on $Al_2O_3$ particles hardens at room temperature, followed by a curing at about 260 °C. The curing effect at constant temperature leads to the small step in the blue curve. The slope of the blue curve is different from the calibration curve. This indicates that the sapphire fiber Bragg grating is strained inside the tube. During heating after curing at about 500 °C the slope of the curve suddenly changes (indicated by the arrow in Fig. 3). The spectra shown in Fig. 2 illustrate this effect more in detail. The fiber Bragg reflection wavelength shifts from 1545.12 nm at 508 °C to 1544.61 nm at 512 °C. This can be explained by losing the force-fit between fiber and tube. The subsequent heating curve (red line) therefore follows the temperature calibration of the fiber. Loosing the mechanical force-fit contact of the first sensor results in a shift of $\Delta\lambda = -0.5$ nm in a temperature range of 4 K between 508 °C and 512 °C. A temperature raise of 4 K was expected to lead to a shift in the Bragg wavelength of +0.1 nm. The measured Bragg wavelength at 512 °C, therefore, differed by –0.6 nm from the expected value.

Using (1) allows to calculate the strain release caused by the shift in the Bragg wavelength of –0.6 nm. From (1), it follows, for the strain contribution, that

$$\varepsilon = \frac{\Delta\lambda}{(\lambda_B \bullet (1-p))}. \tag{3}$$

With $\lambda_B = 1545$ nm and $(1-p) = 0.87$, the shift of 0.6 nm corresponds to a strain release of 450 $\mu$strain. The difference in wavelength between the blue and the green curve of Fig. 3 represents the strain effect. The strain release observed at 512 °C corresponds to about 1/3 of the difference between the green and the blue curve. Thus we assume that about 1/3 of the total strain was released here whereas the residual strain slowly released up to 700 °C, where the green and the blue curves match.

Heating of the fixed sapphire fiber leads to strain imposed by the difference of the thermal expansion coefficients of steel and sapphire $\Delta\alpha$

$$\varepsilon = \Delta T \bullet (\alpha_{\text{steel}} - \alpha_S) = \Delta T \bullet \Delta\alpha. \tag{4}$$

The shift in the Bragg wavelength caused by that strain $\Delta\lambda\varepsilon$ is then given by

$$\Delta\lambda\varepsilon = \lambda_B \bullet (1-p) \bullet \varepsilon = \lambda_B \bullet \Delta\alpha \bullet \Delta T \bullet (1-p). \tag{5}$$

During the measurements of the temperature-dependent shift of the Bragg reflection wavelength, both the spectral shift caused by temperature $\Delta\lambda_T$ and by strain $\Delta\lambda\varepsilon$ are recorded. The pure temperature dependence is determined by the calibration curve of the sapphire fiber. From that the strain is then determined by subtracting the temperature calibration effect from the measured curve.

Linear fits to the curves of Fig. 3 in the temperature range from 250 °C to 500 °C (200 °C to 550 °C for the temperature calibration) result in a slope of 25.4 pm/K for the temperature calibration, 30.1 pm/K during curing and 25.5 pm/K for the subsequent heating. The difference of the thermal expansion therefore leads to a contribution $\Delta\lambda\varepsilon/\Delta T$ of 4.7 pm/K to the sensitivity of the SFBG

$$\frac{\Delta\lambda\varepsilon}{\Delta T} = \lambda_B \bullet \Delta\alpha \bullet (1-p) \tag{6}$$

$$\Delta\alpha = \frac{\left(\frac{\Delta\lambda\varepsilon}{\Delta T}\right)}{(\lambda_B \bullet (1-p))}. \tag{7}$$

From (7), $p = 0.13$ and $\lambda_B = 1532$ nm at room temperature, it follows that $\Delta\lambda = 3.5 \bullet 10^{-6}/$K.

With the given thermal expansion coefficient of sapphire ($\alpha_S = 7.2 \bullet 10^{-6}/$K [22]) the thermal expansion coefficient of the used Inconel tube can be determined to $\alpha_{\text{Inconel}} = 10.7 \bullet 10^{-6}/$K, which is consistent with the literature reported values for Inconel alloys, ranging between 11 and $13 \bullet 10^{-6}/$K [24]. The sapphire fiber was strained to about 1500 $\mu$strain before it lost the force-fit connection.

Thus, the observed strain release of 450 $\mu$strain at 512 °C is about 30%, which confirms the assumptions of the calculation.

## 5.2. Analysis of Second Sensor Design

Fig. 4 shows the temperature characteristics of the second sensor design (see Fig. 1). It is important to note that the metal substrate used for second sensor design was prepared from a special high temperature tough steel alloy containing 9% chromium.

At first, the SFBG was calibrated before it was applied to the sensor pad (green curve). The blue curve was measured during the glassing of the adhesive (DuraSeal). First the curve of the Bragg reflection wavelength follows the temperature calibration up to 600 °C. For $T > 700$ ° C glassing of the adhesive begins, which leads to the desired contact between the steel pad and the sapphire fiber (all features can be seen in Fig. 4). During the subsequent heating cycle after curing (red curve) the temperature dependence differs from the temperature calibration before. As the adhesive reacted at elevated temperatures, the fiber in fact is compressed for temperatures below 350 °C, which is indicated by the fact that the measured Bragg wavelength at 100 °C of the fixed sensor is, at the same temperature, below the calibration Bragg wavelength. Both curves cross at around 350 °C.

From Fig. 4 the linear temperature dependence in the range 100 °C to 600 °C for the fiber was determined to 24.3 pm/K, whereas the fixed sensor shows a slope of 30.1 pm/K.

From the difference of 5.8 pm/K the difference in thermal expansion between sapphire and the steel calculates to $4.3 \bullet 10^{-6}/$K, resulting in an expansion coefficient for the metal of $11.5 \bullet 10^{-6}/$K.

In a next step we used data processing to determine the temperature dependence of the coefficient of thermal expansion (CTE) (see Fig. 5).

The CTE $\alpha_{\text{CTE}}$ is defined as the change of length $l$ of a material at a temperature $T$ with respect to the length at an initial temperature $T_0$ [25]

$$\alpha_{\text{CTE}} = \frac{1}{l(T_0)} \frac{l(T) - l(T_0)}{T - T_0}. \tag{8}$$
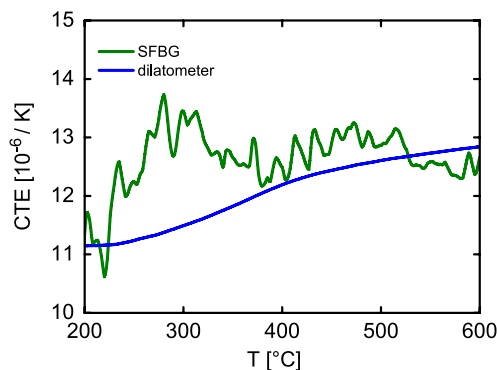
Fig. 5. Temperature dependence of the CTE of the used steel pad determined (green line) by our SFBG-based device and (blue line) by a dilatometer.

A dilatometer is a standard instrument to determine volume or length changes of a specimen at different temperatures, thus given access to information such as the thermal expansion or phase transitions. Similar measurements also can be performed applying fiber Bragg gratings as shown in the following.

The CTE of the steel was calculated from the temperature dependence of the Bragg wavelength shift shown in Fig. 4. For each temperature $\Delta\lambda(T)$ was calculated following the procedure described above. As reference temperature $T_0 = 100°$ C was chosen, as this temperature was fixed at the beginning of the measurements. The CTE of the steel alloy then can be calculated by

$$\alpha_{\text{Steel}}(T) = \Delta\alpha(T) + \alpha_S(T) \tag{9}$$

where $\alpha_S (T)$ is the temperature dependence of the CTE of sapphire in the crystallographic c-direction taken from calibration data for sapphire single crystals [22]. For comparison the thermal expansion coefficient of the used steel was measured by a conventional dilatometer (LinseisL75VD1600C) on a sample with a length of 8 mm also with $T_0 = 100$ °C as reference. Fig. 5 shows the CTE-measurement of both the SFBG and the dilatometer, revealing a fair match between both techniques. The SFBG spectra for the curve were measured in intervals of 60 s. Thus the processing of single spectra was leading to an enhanced noise in the curve. One needs to take into account that the thermal expansion is, in fact, temperature-dependent in the range from 200 °C to 600 °C. However, the fair agreement of both methods proves that indeed SFBGs can be used for remote strain determination.

## 6. Comparison to Glass Fiber Sensors

For SFBG the thermo-mechanic coefficient p is about 0.13 [18], whereas conventional glass fiber based FBG have $p \approx 0.22$ [20], leading to an enhancement in sensitivity in strain sensing of about 10%. On the other hand the temperature dependence for sapphire FBG of about 30 pm/K is three times higher than that for conventional FBGs. Therefore the cross-sensitivity between temperature and strain has to be considered carefully. If the full reflection spectrum can be spectrally resolved, it is indeed possible to determine the Bragg reflection wavelength with a resolution better than 10 pm. This will enables to detect very small strain values of $\Delta l/l < 10^{-5}$. This resolution can be achieved if the temperature is determined within an accuracy of 0.5 K, which, below 700 °C, can be using conventional or fiber optic temperature sensors.

## 7. Summary and Conclusion

We presented high temperature strain measurements using sapphire fiber with inscribed first order fiber Bragg gratings. Two sensor designs were tested up to 600 °C, showing that sapphire Bragg gratings enable the determination of strain with a resolution of about 10 $\mu$strain. The

maximum applied strain was 1500 $\mu$strain without any indication of sensor failure. Using our sensors the thermal expansion coefficients of two different metals were measured even as function of temperature. Further improvement on sensor design and packaging as well on signal processing will further improve the performance of SFBG strain sensors, which might represent a flexible alternative to currently used high temperature strain gauges.

## References

[1] J. Buggea, S. Kjaera, and R. Blumb, "High-efficiency coal-fired power plants development and perspectives," *Energy*, vol. 31, no. 10/11, pp. 1437–1445, Aug. 2006.

[2] P. Chiesa and E. Macchi, "A thermodynamic analysis of different options to break 60% electric efficiency in combined cycle power plants," *J. Eng. Gas Turbines Power*, vol. 126, no. 4, pp. 770–785, Nov. 2004.

[3] R. Viswanathan, K. Coleman, and U. Rao, "Materials for ultra-supercritical coal-fired power plant boilers," *Int. J. Pressure Vessels Piping*, vol. 83, no. 11/12, pp. 778–783, Nov./Dec. 2006.

[4] M. Woike, A. Abdul-Aziz, N. Oza, and B. Matthews, "New sensors and techniques for the structural health monitoring of propulsion systems," *Sci. World J.*, vol. 2013, 2013, Art. no. 596506.

[5] W. Ecke, I. Latka, R. Willsch, A. Reutlinger, and R. Graue, "Fibre optic sensor network for spacecraft health monitoring," *Meas. Sci. Technol.*, vol. 12, no. 7, pp. 974–980, Apr. 2001.

[6] *Catalogue Strain Gauges*, Tokyo Sokki Kenkyujo Co., Ltd., Tokyo, Japan, 2015.

[7] J. Maul and T. Kipp, "*Sensing of surface strain with flexible fiber Bragg strain gages*," 2011. [Online]. Available: hbm.com

[8] Accessed Feb. 24, 2016. [Online]. Available: http://www.fbgs.com/applications/strain-sensing/

[9] Accessed Feb. 24, 2016. [Online]. Available: http://www.zse.de/index.cfm/content/products/product/OptischeDehnungsmessstreifen und Sensoren.cfm

[10] S. J. Mihailov, "Fiber Bragg grating sensors for harsh environments," *Sensors*, vol. 12, no. 2, pp. 1898–1918, Feb. 2012.

[11] P. Moyo, J. M. W. Brownjohn, R. Suresh, and S. C. Tjin, "Development of fiber Bragg grating sensors for monitoring civil infrastructure," *Eng. Struct.*, vol. 27, no. 12, pp. 1828–1834, Oct. 2005.

[12] J. Canning, S. Bandyopadhyay, M. Stevenson, and K. Cook, "Fiber Bragg grating sensor for high temperature application," in *Proc. Joint Conf. Opto-Electron. Commun. Conf. Australian Conf. Opt. Fibre Technol.*, Sydney, Australia, Jul. 7–10, 2008, pp. 1–2.

[13] E. Lindner *et al.,* "Post-hydrogen-loaded draw tower fiber Bragg gratings and their thermal regeneration," *Appl. Opt.*, vol. 50, no. 17, pp. 2519–2522, Jun. 2011.

[14] Y. Rao, Z. Ran, X. Liao, and H. Deng, "Hybrid LPFG/MEFPI sensor for simultaneous measurement of high-temperature and strain," *Opt. Exp.*, vol. 15, no. 22, pp. 14 936–14 941, 2007.

[15] D. Grobnic, S. J. Mihailov, C. W. Smelser, and H. Ding, "Sapphire fiber Bragg grating sensor made using femtosecond laser radiation for ultrahigh temperature applications," *IEEE Photon. Technol. Lett.*, vol. 16, no. 11, pp. 2505–2507, Nov. 2004.

[16] M. Busch *et al.,* "Inscription and characterization of Bragg gratings in single-crystal sapphire optical fibres for high-temperature sensor applications," *Meas. Sci. Technol.*, vol. 20, no. 11, Oct. 2009, Art. no. 115301.

[17] T. Habisreuther *et al.,* "Sapphire fiber Bragg gratings for high temperature and dynamic temperature diagnostics," *Appl. Therm. Eng.*, vol. 91, pp. 860–865, Dec. 2015.

[18] S. Mihailov, D. Grobnic, and C. Smelser, "High-temperature multiparameter sensor based on sapphire fiber Bragg gratings," *Opt. Lett.*, vol. 35, no. 16, pp. 2810–2812, Aug. 2010.

[19] T. Elsmann, T. Habisreuther, A. Graf, M. Rothhardt, and H. Bartelt, "Inscription of first-order sapphire Bragg gratings using 400 nm femtosecond laser radiation," *Opt. Exp.*, vol. 21, no. 4, pp. 4591–4597, Feb. 2013.

[20] A. D. Kersey *et al.,* "Fiber grating sensors," *J. Lightw. Technol.*, vol. 15, no. 8, pp. 1442–1463, Aug. 1997.

[21] T. Habisreuther *et al.,* "Optical sapphire fiber Bragg gratings as high temperature sensors," in *Proc. SPIE*, May 2013, vol. 8794, pp. 1–4.

[22] *Certificate of Compliance on Certification of Standard Sample From Reference Material of Linear Thermal Expansion Coefficient Made From Monocrystal Aluminium Oxide*, D. I. Mendeleyev Inst. Metrology (VNIIM), St. Petersburg, Russia, 2004.

[23] T. Elsmann, T. Habisreuther, M. Rothhardt, R. Willsch, and H. Bartelt, "Advanced fabrication and calibration of high-temperature sensor elements based on sapphire fiber Bragg gratings," in *Proc. SPIE*, Jun. 2014, vol. 9157, pp. 1–4.

[24] last visit Feb. 24, 2015. [Online]. Available: http://www.specialmetals.com/alloys

[25] *Glas—Bestimmung des Mittleren Thermischen Längenausdehnungskoeffizienten*, DIN ISO 7991, DIN Deutsches Inst. Normung e. V., 2005